Research Article

Journal of PeptideScience

Received: 28 September 2011 Revised: 3 November 2011 Accepted: 15 November 2011 Published online in Wiley Online Library: 16 January 2012

(wileyonlinelibrary.com) DOI 10.1002/psc.1439

Antimicrobial activity of peptides derived from human ß-amyloid precursor protein

Praveen Papareddy,[a] Matthias Mörgelin,[c] Björn Walse,[d] Artur Schmidtchen[a] and Martin Malmsten[b]*

Antimicrobial peptides are important effector molecules of the innate immune system. Here, we describe that peptides derived from the heparin-binding disulfide-constrained loop region of human ß-amyloid precursor protein are antimicrobial. The peptides investigated were linear and cyclic forms of NWCKRGRKQCKTHPH (NWC15) as well as the cyclic form comprising the C-terminal hydrophobic amino acid extension FVIPY (NWCKRGRKQCKTHPHFVIPY; NWC20c). Compared with the benchmark antimicrobial peptide LL-37, these peptides efficiently killed the Gram-negative bacteria *Escherichia coli* and *Pseudomonas aeruginosa*, the Gram-positive *Staphylococcus aureus* and *Bacillus subtilis*, and the fungi *Candida albicans* and *Candida parapsilosis*. Correspondingly, fluorescence and electron microscopy demonstrated that the peptides caused defects in bacterial membranes. Analogously, the peptides permeabilised negatively charged liposomes. Despite their bactericidal effect, the peptides displayed very limited hemolytic activities within the concentration range investigated and exerted very small membrane permeabilising effects on human epithelial cells. The efficiency of the peptides with respect to bacterial killing and liposome membrane leakage was in the order NWC20c > NWC15c > NWC15l, which also correlated to the adsorption density for these peptides at the model lipid membrane. Thus, whereas the cationic sequence is a minimum determinant for antimicrobial action, a constrained loop-structure as well as a hydrophobic extension further contributes to membrane permeabilising activity of this region of amyloid precursor protein. Copyright © 2012 European Peptide Society and John Wiley & Sons, Ltd.

Keywords: antimicrobial; APP; bacteria; liposomes; membrane; peptide

Introduction

Many antimicrobial peptides (AMPs) are characterized by an amphipathic structure, where stretches of hydrophobic and cationic amino acids are spatially organized in sectors of the molecules. For example, AMPs comprise linear peptides, many of which may adopt α-helical and amphipathic conformation upon bacterial binding, peptides forming cysteine-linked antiparallel β-sheets, as well as cysteine-constrained loop structures. Other AMPs are characterized by an over-representation of certain amino acids [1–6]. Although the interaction with bacteria and their membranes is a prerequisite for AMPs, the modes of action of AMPs are complex, involving membrane disruption as well as non-lytic mechanisms [1,3,7,8].

In many cases, AMPs are multifunctional, and the biological effects exerted by these molecules include, e.g. growth stimulus and angiogenesis, protease inhibition, anti-angiogenesis, and chemotaxis [9–11]. These multiple roles of AMPs reflect their ability to interact with negatively charged glycosaminoglycans, biomembranes, and various cell receptors, including formyl-peptide receptors and Toll-like receptors [12,13]. Correspondingly, cationic peptide sequences of many endogenous proteins exert antimicrobial activities. For example, complement C3 [14]; kininogen [15,16]; heparin-binding protein [17]; heparin-binding epidermal growth factor and other growth factors [18]; matrix proteins such as laminin, fibronectin, and proline arginine-rich end leucine-rich repeat protein; prions [19]; β2-glycoprotein [20]; histidine-rich glycoprotein [21]; thrombin [22]; chromogranins [23,24]; and tissue factor pathway inhibitor [25] may, either as holoproteins or smaller peptide derivatives thereof, also exert antimicrobial activities *in vitro* and, in several cases, *in vivo* [15,16,21]. These findings are compatible with the observation that consensus heparin-binding peptide sequences (Cardin and Weintraub motifs) XBBBXXBX or XBBXBX (where X represents hydrophobic or uncharged amino acids, and B represents basic amino acids), including multiples of the motifs ARKKAAKA or AKKARA [26], are antibacterial [27] and interact with membranes [28].

These findings indicate that endogenous peptides derived from various proteins may exert activities similar to 'classical' AMPs. The ß-amyloid precursor protein (APP) is an integral membrane protein most known for one of its proteolytic breakdown products, ß-amyloid, a major component of the diffuse and fibrillar deposits found in Alzeimer's disease [29,30]. The normal physiological role of APP remains largely unknown despite much work. The predominant isoform of APP consists of a large extracellular region, a transmembrane region, and a small cytoplasmic part. The N-terminal domain is well characterized and has been shown to act as a possible growth factor [31]. Electrostatic calculations indicate that there is a highly positively charged surface

* *Correspondence to: Martin Malmsten, Department of Pharmacy, Uppsala University, SE-751 23 Uppsala, Sweden. E-mail: martin.malmsten@farmaci.uu.se*

a *Division of Dermatology and Venereology, Department of Clinical Sciences, Lund University, Biomedical Center, Tornavägen 10, SE-221 84 Lund, Sweden*

b *Department of Pharmacy, Uppsala University, SE-751 23 Uppsala, Sweden*

c *Division of Infection Medicine, Department of Clinical Sciences, Lund University, Biomedical Center, Tornavägen 10, SE-221 84 Lund, Sweden*

d *SARomics AB, SE-220 07 Lund, Sweden*

on one side of the APP N-terminal domain, centered about the disulfide Cys 98 to Cys 105, and including a peptide region that has previously been identified as a heparin-binding site. The surface of the positive patch is dominated by the β-hairpin loop (residues 96–110). There is, furthermore, a large hydrophobic patch immediately adjacent to the heparin-binding region, with Met 36, Phe 37, Ile 69, Pro 109, Val 112, Ile 113, and Tyr 115 as major contributors. Considering its amphiphilic nature, it has been hypothesized that this surface may be involved in mediating various functions, including protein binding and dimerization [31].

The aforementioned observations, together with previous findings that APP generates several bioactive fragments on proteolytic degradation [32] and that another region of APP, i.e. amyloid β [33], displays antimicrobial properties, prompted us to investigate whether this region of APP may exert activity against bacteria. Bacterial permeabilization by synthetic peptides, encompassing the heparin-binding region, was further investigated by using liposome assays, and by ellipsometry, circular dichroism (CD), and fluorescence spectroscopy. Additionally, effects of the peptides were tested on erythrocytes and epithelial cells. The results demonstrate that the heparin-binding region of APP may indeed exert antimicrobial effects similar to 'classical' AMPs.

Materials and Methods

Materials

The linear and cyclic forms of NWC15 (NWCKRGRKQCKTHPH), NWC15l and NWC15c, respectively, and the longer cyclic NWCKRGRKQCKTHPHFVIPY (NWC20c) (cyclication for both NWC15c and NWC20c obtained through the cysteine groups) and LL-37 (LLGDFFRKSKEKIGKEFKRIVQRIKDFLRNLVPRTES) were synthesized by Innovagen AB (Lund, Sweden). The purity of the peptides was >95% in all cases, as confirmed by reverse phase HPLC and matrix-assisted laser desorption/ionization time-of-flight mass spectrometry analysis (Voyager, Applied Biosystems).

Microorganisms

Escherichia coli ATCC 25922, *Pseudomonas aeruginosa* ATCC 27853, *Bacillus subtilis* ATCC 6633, *Staphylococcus aureus* ATCC 29213, *Candida albicans* ATCC 90028, and *Candida parapsilosis* ATCC 90018 were all obtained from the Department of Clinical Bacteriology at Lund University Hospital.

Viable Count Analysis

Escherichia coli bacteria were grown to mid-logarithmic phase in Todd–Hewitt (TH) medium. Bacteria were washed and diluted in 10 mM Tris, pH 7.4, containing 5 mM glucose, 0.15 M NaCl, 20% human citrate plasma. Bacteria (50 µl; 2×10^6 cfu/ml) were incubated at 37 °C for 2 h, with the synthetic peptides at a concentration of 30 and 60 µM. To quantify the bactericidal activity, serial dilutions of the incubation mixture were plated on TH agar, followed by incubation at 37 °C overnight and determination of the number of colony-forming units (cfu).

Radial Diffusion Assay

Radial diffusion assay (RDA) measurements were performed essentially as described earlier [34]. Briefly, bacteria were grown to mid-logarithmic phase in 10 ml of full-strength (3% w/v) trypticase soy broth (TSB) (Becton-Dickinson, Cockeysville, MD). The microorganisms were washed once with 10 mM Tris, pH 7.4. After this, 4×10^6 bacterial cfu was added to 5 ml of the underlay agarose gel, consisting of 0.03% (w/v) TSB, 1% (w/v) low-electroendosmosistype agarose (Sigma, St Louis MO), and a final concentration of 0.02% (v/v) Tween 20 (Sigma). The underlay was poured into a Ø 85-mm petri dish. After agarose solidification, 4-mm-diameter wells were punched and 6 µl of test sample added to each well. Plates were incubated at 37 °C for 3 h to allow peptide diffusion. The underlay gel was then covered with 5 ml of molten overlay (6% TSB and 1% low-electroendosmosistype agarose in dH_2O). Antimicrobial activity of a peptide was visualized as a clear zone around each well after 18–24 h of incubation at 37 °C. Synthetic peptides were tested at 100 µM to determine the antibacterial effect relative to the benchmark peptide LL-37. Although MIC investigations under various standardized protocols can of course be used as well, these also suffer from shortcomings, e.g. related to the presence of polyanionic species (e.g. peptides and polysaccharides) originating from physiologically less relevant components such as casein hydrolysate, beef extract, and starch, used in the growth medium [35]. This points to the need to monitor the antimicrobial activity of AMPs also in physiologically more relevant settings, e.g. in whole blood or at least in serum or plasma, which was one of the reasons for including antimicrobial activity data for one of the bacteria (*E. coli*) also in the presence of plasma, using viable count assay (VCA). However, because the purpose of the present investigation was merely to demonstrate an antimicrobial effect and to compare this with that of the well-known benchmark LL-37, the combination of RDA and VCA measurements is sufficient, particularly because previous studies in literature [36] have demonstrated a close correlation between RDA, VCA, and MIC variations within peptide analogue series, as well as between bacteria killing with these assays and membrane rupture effects observable by electron spectroscopy.

Liposome Preparation and Leakage Assay

As model lipid membranes, anionic DOPE/DOPG (75/25 mol/mol) liposomes were used. DOPG (1,2-dioleoyl-*sn*-Glycero-3-phosphoglycerol, monosodium salt) and DOPE (1,2-dioleoyl-*sn*-Glycero-3-phoshoetanolamine) were both from Avanti Polar Lipids (Alabaster, USA) and of >99% purity. The lipid mixture was dissolved in chloroform; after which solvent was removed by evaporation under vacuum overnight. Subsequently, 10 mM Tris buffer, pH 7.4, was added together with 0.1 M carboxyfluorescein (CF) (Sigma, St. Louis, USA). After hydration, the lipid mixture was subjected to eight freeze–thaw cycles consisting of freezing in liquid nitrogen and heating to 60 °C. Unilamellar liposomes of about Ø140 nm were generated by multiple extrusions (30 passages) through polycarbonate filters (pore size 100 nm) mounted in a Lipo-Fast miniextruder (Avestin, Ottawa, Canada) at 22 °C. Untrapped CF was removed by two subsequent gel filtrations (Sephadex G-50, GE Healthcare, Uppsala, Sweden) at 22 °C, with Tris buffer as eluent. CF release from the liposomes was determined by monitoring the emitted fluorescence at 520 nm from a liposome dispersion (10 µM lipid in 10 mM Tris, pH 7.4). An absolute leakage scale was obtained by disrupting the liposomes at the end of each experiment through addition of 0.8 mM Triton X-100 (Sigma-Aldrich, St. Louis, USA). A SPEX-fluorolog 1650 0.22-m double spectrometer (SPEX Industries, Edison, USA) was used for the liposome leakage assay. Measurements were performed in triplicate at 37 °C.

Journal of PeptideScience

Fluorescence Microscopy

For study of membrane permeabilization using the impermeant probe fluorescein isothiocyanate (FITC), *E. coli* bacteria were grown to mid-logarithmic phase in TSB medium. The bacteria were washed and resuspended in 10 mM Tris, pH 7.4, containing also 10 mM glucose to yield a suspension of 1×10^7 cfu/ml. Hundred microliters of the bacterial suspension was incubated with 30 μM of the respective peptides at 30 °C for 30 min. Microorganisms were then immobilized on poly(L-Lys)-coated glass slides by incubation for 45 min at 30 °C, followed by addition onto the slides of 200 μl of FITC (6 μg/ml) in the appropriate buffers, and incubated for 30 min at 30 °C. The slides were washed and bacteria fixed by incubation, first on ice for 15 min and then at room temperature for 45 min in 4% paraformaldehyde. The glass slides were subsequently mounted on slides by using Prolong Gold antifade reagent mounting medium (Invitrogen). For fluorescence analysis, bacteria were visualized by using a Nikon Eclipse TE300 (Nikon, Melville, NY) inverted fluorescence microscope equipped with a Hamamatsu C4742-95 cooled charge-coupled device camera (Hamamatsu, Bridgewater, MJ) and a Plan Apochromat × 100 objective (Olympus, Orangeburg, NY). Differential interference contrast (Nomarski) imaging was used for visualization of the microbes themselves.

Fluorescence Spectroscopy

Tryptophan fluorescence spectra were determined by a SPEX Fluorolog-2 spectrofluorometer at a peptide concentration of 10 μM. An excitation wavelength of 280 nm was used, whereas emission spectra were taken between 300 and 450 nm. Measurements were conducted at 37 °C while stirring in 10 mM Tris, pH 7.4. Where indicated, liposomes (100 μM lipid) were included, incubated with the peptides for 1 h before measurements were initiated. Spectra intensities were normalized to those for 10 mM Tris, pH 7.4, to facilitate comparison of spectral maximum positions.

Electron Microscopy

For transmission electron microscopy and visualization of peptide effects on bacteria, *P. aeruginosa* and *S. aureus* ($1–2 \times 10^6$ cfu/sample) were incubated for 2 h at 37 °C with the peptides (30 μM). Samples of *P. aeruginosa* and *S. aureus* suspensions were adsorbed onto carbon-coated copper grids for 2 min, washed briefly with two drops of water, and negatively stained with two drops of 0.75% uranyl formate. The grids were rendered hydrophilic by glow discharge at low pressure in air. All samples were examined with a Jeol JEM 1230 (Jeol, Tokyo, Japan) electron microscope operated at 80 kV accelerating voltage. Images were recorded with a Gatan Multiscan 791 (Gatan, Pleasanton, CA) charge-coupled device camera.

CD Spectroscopy

Circular dichroism spectra were measured by a Jasco J-810 Spectropolarimeter (Jasco, Easton, USA). The measurements were performed in duplicate at 37 °C in a 10-mm quartz cuvette under stirring with a peptide concentration of 10 μM. The effect on peptide secondary structure of liposomes at a lipid concentration of 100 μM was monitored in the range 200–260 nm. To account for instrumental differences between measurements as well as signals from bulk solution, background substraction was performed routinely.

Hemolysis Assay

EDTA-blood was centrifuged at 800 *g* for 10 min, and plasma and buffy coat removed. Erythrocytes were washed three times and resuspended in 5% phosphate buffer saline, pH 7.4. The cells were then incubated with end-over-end rotation for 1 h at 37 °C in the presence of different concentrations of peptide (0, 3, 6, 30, 60 μM). For comparison, LL-37 was investigated at the same concentrations. Two percent Triton X-100 served as positive control. The samples were then centrifuged at 800 *g* for 10 min. The absorbance of hemoglobin release was measured at 540 nm and is expressed as % of Triton X-100 induced hemolysis.

Lactate Dehydrogenase (LDH) Assay

HaCaT keratinocytes were grown to confluency in 96 well plates (3000 cells/well) in serum-free keratinocyte medium (SFM) supplemented with bovine pituitary extract and recombinant EGF (BPE-rEGF) (Invitrogen, Eugene, USA). The medium was then removed, and 100 μl of the peptides investigated (at 60 μM, diluted in SFM/BPE-rEGF or in keratinocyte-SFM supplemented with 20% human serum) was added. The LDH-based TOX-7 kit (Sigma-Aldrich, St. Louis, USA) was used for quantification of LDH release from the cells. Results represent mean values from triplicate measurements and are given as fractional LDH release compared with the positive control consisting of 1% Triton X-100 (yielding 100% LDH release).

MTT Assay

Sterile-filtered MTT (3-(4,5-dimethylthiazolyl)-2,5-diphenyl-tetrazoliumbromide; Sigma-Aldrich, St. Louis, USA) solution (5 mg/ml in phosphate buffer saline (PBS)) was stored protected from light at −20 °C until usage. HaCaT keratinocytes, 3000 cells/well, were seeded in 96 well plates and grown in keratinocyte-SFM/BPE-rEGF medium to confluence. Keratinocyte-SFM/BPE-rEGF medium alone, or keratinocyte-SFM supplemented with 20% serum, was added, followed by peptide addition to 60 μM. After incubation over night, 20 μl of the MTT solution was added to each well and the plates incubated for 1 h in CO_2 at 37 °C. The MTT-containing medium was then removed by aspiration. The blue formazan product generated was dissolved by the addition of 100 μl of 100% DMSO per well. The plates were then gently swirled for 10 min at room temperature to dissolve the precipitate. The absorbance was monitored at 550 nm, and results given represent mean values from triplicate measurements.

Ellipsometry

Peptide adsorption to supported lipid bilayers was studied *in situ* by null ellipsometry, using an Optrel Multiskop (Optrel, Kleinmachnow, Germany) equipped with a 100 mW argon laser. All measurements were carried out at 532 nm and an angle of incidence of 67.66° in a 5-ml cuvette under stirring (300 rpm). Both the principles of null ellipsometry and the procedures used have been described extensively before [37,38]. In brief, by monitoring the change in the state of polarization of light reflected at a surface in the absence and presence of an adsorbed layer, the mean refractive index (n) and layer thickness (d) of the adsorbed layer can be obtained. From the thickness and refractive index, the adsorbed amount (Γ) was calculated according to [39]:

$$\Gamma = \frac{(n - n_0)}{dn/dc} d \quad (1)$$

where dn/dc is the refractive index increment (0.154 cm^3/g) and n_0 is the refractive index of the bulk solution. Corrections were

routinely performed for changes in bulk refractive index caused by changes in temperature and excess electrolyte concentration.

Supported lipid bilayers were generated from liposome adsorption to silica surfaces (electric surface potential −40 mV and contact angle of <10°) [40]. DOPE/DOPG (75/25 mol/mol) liposomes were prepared as described earlier, but the dried film resuspended in Tris buffer containing no CF. To avoid adsorption of peptide directly at the silica substrate through any defects of the supported lipid layer, poly-L-Lys (M_w = 170 kDa, Sigma-Aldrich, St Louis, USA) was pre-adsorbed from water prior to lipid addition to an amount of 0.045 ± 0.01 mg/m^2, followed by removal of nonadsorbed poly-L-Lys by rinsing with water at 5 ml/min for 20 min. Water contained in the cuvette was then replaced by buffer containing also 150 mM NaCl, which was followed by addition of liposomes in buffer at a lipid concentration of 20 μM, and subsequently by rinsing with buffer (5 ml/min for 15 min) when the liposome adsorption had stabilized. The final layer formed had structural characteristics (thickness 4 ± 1 nm, mean refractive index 1.47 ± 0.026) suggesting that a layer fairly close to a complete bilayer is formed. Again, the bilayer build-up was performed at 25 °C.

After lipid bilayer formation, temperature was raised and the cuvette content replaced by 10 mM Tris buffer at a rate of 5 ml/min over a period of 30 min. After stabilization for 40 min, peptide was added to a concentration of 0.01 μM, followed by three subsequent peptide additions to 0.1, 0.5, and 1 μM, in all cases monitoring the adsorption for 1 h. All measurements were made in at least duplicate.

Throughout, data are shown in figures as mean values ± standard deviations.

Results

Antibacterial Activities of APP-derived Peptides

First, we investigated the effects of the APP-derived peptides NWC15l, NWC15c, and NWC20c on bacteria and fungi. The peptides were found to be antibacterial and antifungal in radial diffusion assays (RDA) by using the Gram-negative bacteria *E. coli* and *P. aeruginosa*, the Gram-positive bacteria *S. aureus* and *B. subtilis*, and the fungi *C. albicans* and *C. parapsilosis* (Figure 1).

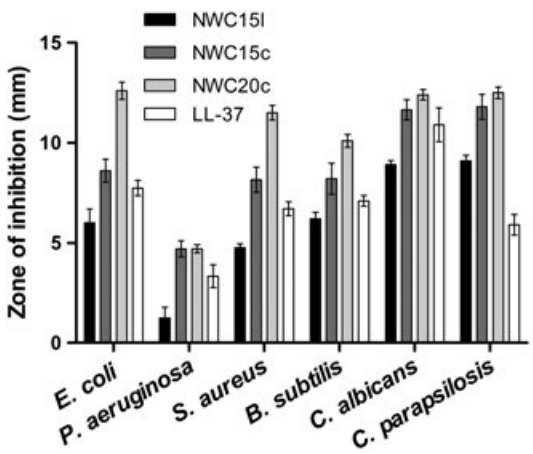

Figure 1. Antibacterial activities of the indicated APP-derived peptides. For determination of antibacterial activities, the indicated bacterial or fungal isolates (4 × 10^6 cfu) were inoculated in 0.1% TSB agarose gel. Each 4-mm-diameter well was loaded with 6 μl of peptide (at 100 μM). The zones of clearance correspond to the inhibitory effect of each peptide after incubation at 37 °C for 18–24 h (mean values are presented, n = 3).

The efficiency of the peptides with respect to microbial killing was, in general, in the order NWC20c > NWC15c > NWC15l. Noteworthy, NWC20c yielded similar or larger inhibition zones when compared with the classical 'benchmark' AMP LL-37. To further explore the effects of these peptides in physiologically relevant environments (although physiological concentrations of APP-based peptides are presently unknown), VCAs in presence of 0.15 M NaCl and 20% human citrate plasma were performed against *E. coli* (Figure 2). In analogy to the aforementioned experiments, data showed that NWC20c retained antimicrobial effects in this environment, whereas both NWC15l and NWC15c showed substantially weaker antibacterial effect.

Permeabilization and Electron Microscopy Studies

Figure 3(A) shows that the APP-derived peptides permeabilized *E. coli* bacteria, as visualized with the impermeant probe FITC. To further examine peptide-induced permeabilization of different bacterial plasma membranes, *P. aeruginosa* and *S. aureus* were incubated with 30 μM of peptide, yielding complete bacterial killing in 10 mM Tris, pH 7.4 and 10 mM glucose, and analyzed by electron microscopy (Figure 3(B)). Clear differences in morphology between peptide-treated bacteria and the untreated control were demonstrated. Florescence and electron microscopy revealed that, similarly to LL-37, the APP peptides caused local perturbations and breaks along *E. coli*, *P. aeruginosa*, and *S. aureus* plasma membranes, and intracellular material was found extracellularly.

Effects on Human Cells

Despite their antimicrobial effects, no hemolytic activity of the APP-derived peptides was detected at doses of 3–60 μM (Figure 4 (A)). This contrasted to the antimicrobial peptide LL-37, which permeabilised erythrocytes at 60 μM. Analogously, the APP-derived peptides did not permeabilize human epithelial cells at this concentration (HaCaT keratinocyte cell line) and correspondingly did not affect viability (Figure 4(B)).

Of course, the results obtained with these assays do not fully predict toxicity of the peptides investigated and only apply to the concentration range and conditions used, and no claims can be made for higher concentrations, or for toxicity in other cell lines, in various animal models, etc. Instead, the main point enabled through the use of these toxicity assays is the comparison with the negative control and with the widely investigated benchmark AMP LL-37 within this concentration range.

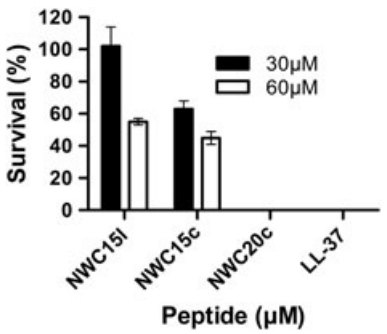

Figure 2. Effect of peptides in presence of physiological conditions. Antibacterial effects of the indicated peptides against *E. coli* in VCA are presented. Bacteria were incubated in 50 μl with the indicated peptides at either 30 or 60 μM in 10 mM Tris, pH 7.4, 0.15 M NaCl, 20% human citrate plasma. Identical buffers without peptides were used as controls.

Journal of PeptideScience

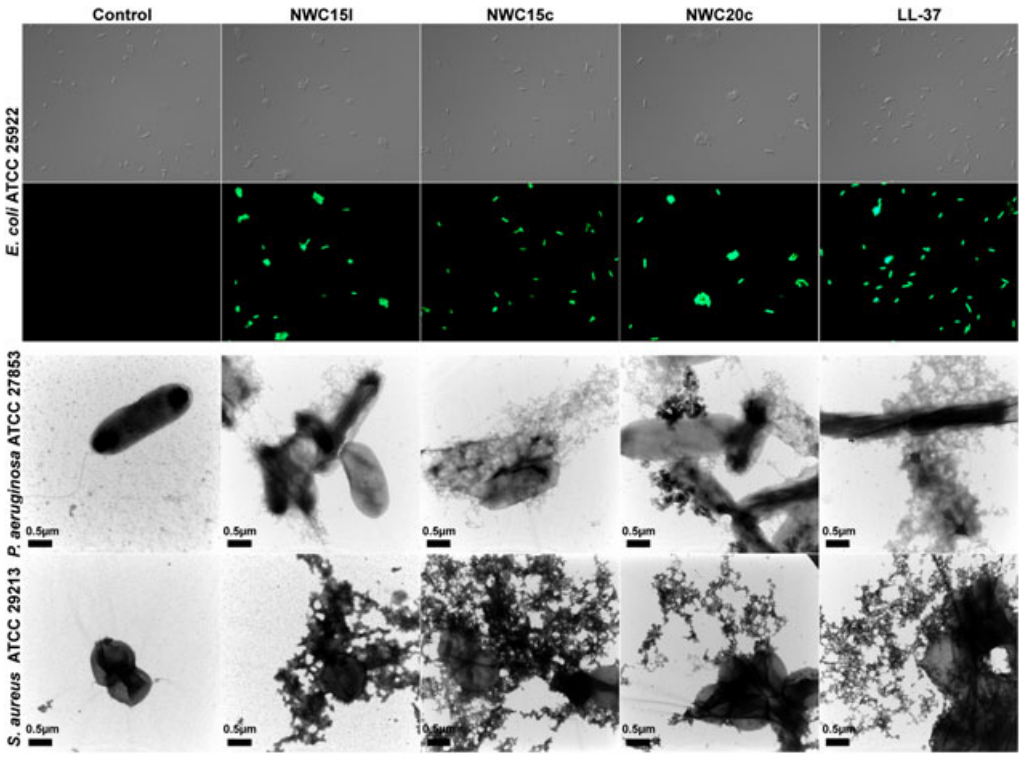

Figure 3. Permeabilization effects. (A) Permeabilizing effects of peptides on *E. coli*. Bacteria were incubated with the indicated peptides, and permeabilization was assessed by using the impermeant probe FITC. (B) Electron microscopy analysis. *P. aeruginosa* and *S. aureus* bacteria were incubated for 2 h at 37 °C with 30 μM of the APP-derived peptides and analyzed with electron microscopy. Results for LL-37 is also included for comparison. Scale bar represents 0.5 μm.

Model Membrane Interaction

Addressing the issue of peptide-binding to model DOPE/DOPG membranes, W fluorescence spectroscopy measurements were monitored in buffer with and without liposomes present. As can be seen in Figure 5, there are only very minor differences between the spectra. Because W fluorescence is highly sensitive to the polarity of the ambient [41], the emission peak at ≈360 nm shows that the W residues of membrane-bound NWC15l, NWC15c, and NWC20c are all exposed to the aqueous solution. Furthermore, CD spectroscopy demonstrates that there is little or no helix induction in these peptides in the presence of the phospholipid membrane (Figure 6), excluding ordered transmembrane structures. In contrast, LL-37 displays a pronounced helix induction on interaction with negatively charged lipid membranes. Taken together, fluorescence and CD spectroscopy shows that the APP peptides investigated bind to phospholipid membranes within, or close to, the polar headgroup region in the membrane. This is in agreement with previous findings that bulky and polarizable W residues have an affinity to interfaces and are frequently located in the proximity of the polar headgroup region in phospholipid membranes [42–48].

As previously demonstrated, e.g. for peptides derived from kininogen, end-tagging by hydrophobic amino acid stretches promotes peptide-binding to phospholipid membranes, resulting in increased membrane lysis in both model lipid liposomes and bacteria [36]. The same applies also to the presently investigated APP-derived peptides, where NWC20c (NW**C**KRGRKQ**C**KTHPHFVIPY) induces significantly more pronounced leakage in liposomes than the 'non-tagged' NWC15 peptides (NW**C**KRGRKQ**C**KTHPH) (Figure 7). In parallel, NWC20c adsorption is significantly higher than that of NWC15l and NWC15c (Figure 8), clearly a result of the lack of the hydrophobic anchor tail in the latter cases (Figure 9). Here, we also note that NWC15c displays a slightly higher binding than NWC15l to the DOPE/DOPG membranes and causes a slightly larger liposome leakage induction, in agreement with the findings of a higher antimicrobial activity of NWC15c.

Discussion

The main findings from the present study is the identification of an antimicrobial epitope representing a heparin-binding region of APP, paired with the observation that a cylic structure, together with an adjacent hydrophobic amino acid stretch, is needed for optimal activity of this region. This further substantiates the concept presented in our previous work [14,15,27,49], showing that various endogenous proteins harbour 'cryptic' epitopes that display antimicrobial properties. Furthermore, the data suggest that a constrained cyclic structure, such as represented by NWC20c and NWC15c, presents an optimized surface enabling interactions with the lipid membranes of bacteria (Figure 8).

The finding of an increased membrane-binding and membrane-disrupting capacity of NWC20c compared with the NWC15 peptides is analogous to previous findings for AMPs end-tagged with hydrophobic acyl groups [50,51] or with hydrophobic amino acid stretches [36]. For such modified AMPs, hydrophobic interactions facilitate membrane-binding, also at high ionic strength and in the presence of serum, as well as efficient membrane lysis and antimicrobial properties. For W-tagged and F-tagged AMPs, the end-tagging furthermore contributes to selectivity between bacteria/fungi and mammalian cells [52]. The latter is because of both charge density differences between these membranes and the

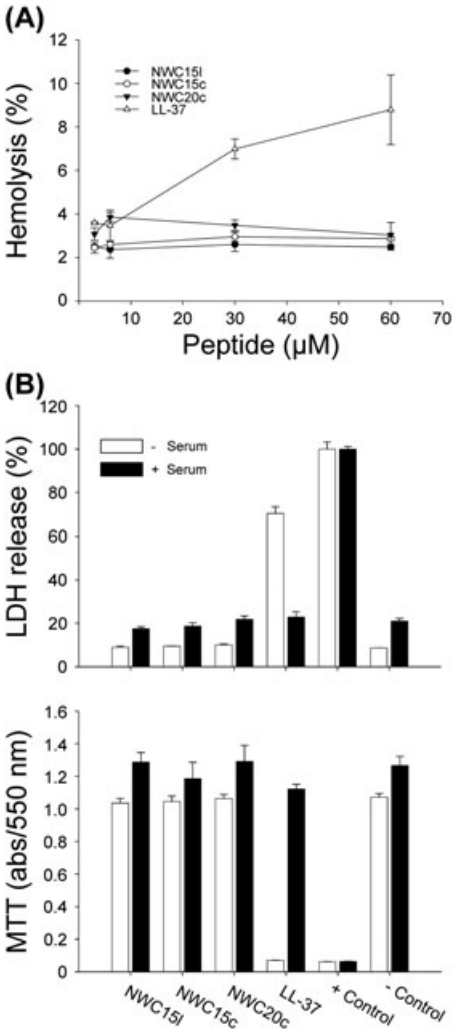

Figure 4. (A) Hemolytic effects of the indicated APP peptides were investigated, and corresponding data for LL-37 were included for comparison. The cells were incubated with the peptide concentrations at 3, 6, 30, and 60 μM, 2% Triton X-100 serving as positive control. The absorbance of hemoglobin released was measured at 540 nm and is expressed as % of Triton X-100 induced hemolysis (note scale of *y*-axis). (B) Effects of peptides at 60 μM on HaCaT cells in absence (open bars) and presence (filled bars) of human serum. Cell permeabilizing effects of the indicated peptides (upper panel) were measured by the LDH-based TOX-7 kit. LDH release from the cells was measured at 490 nm and was plotted as % of total LDH release. The MTT assay (lower panel) was used to measure viability of HaCaT keratinocytes. In the assay, MTT is modified into a dye, blue formazan, by enzymes associated with metabolic activity. The absorbance of the dye was measured at 550 nm.

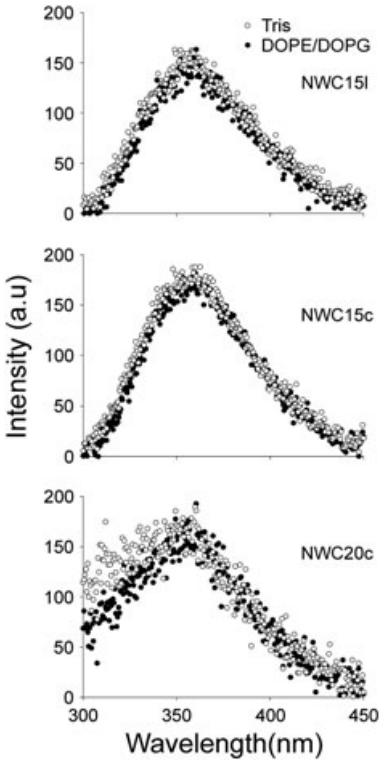

Figure 5. Tryptophan fluorescence spectra, at a peptide concentration of 10 μM, for the indicated peptides in 10 mM Tris, pH 7.4, in the presence and absence of DOPE/DOPG (75/25 mol/mol) liposomes (100 μM lipid).

bulkiness of the W/F residues, which result in a large free energy penalty on membrane incorporation, particularly in the presence of membrane-condensing cholesterol, as in mammalian cells. Although more complex than the W-tags and F-tags previously investigated, the F and Y residues of the FVIPY 'tag' of NWC20c are expected to cause qualitatively similar effects as the previously investigated W and F oligopeptide tags.

Notable in this context is, furthermore, a slightly higher membrane-disrupting capacity of NWC15c than of NWC15l in liposomes, which parallels a higher antimicrobial effect of this peptide in the RDA experiments. Also in parallel to this, adsorption of NWC15c at the DOPE/DOPG membrane is higher than that of NWC15l. Here, it is interesting to note some previous studies in literature on the effect of cyclization on the interaction between peptides and oppositely charged surfaces and lipid membranes. For example, Seker *et al.* investigated adsorption of cyclic and linear variants of the Pt-binding peptide PTSTGQA and found the cyclic peptide to display substantially higher adsorption at Pt/Au than the linear one [53]. Analogous results were found by Ringstad *et al.* for linear and cyclic variants of the kininogen-derived peptide HKH20 [54]. At the same time, however, a comparable membrane-disrupting capacity was found for the linear and cyclic peptide variants in the latter study, which was interpreted as being a result of facilitated close charge–charge contacts for the linear peptide when bound to the lipid membrane. In analogy to the latter observation, several investigators [53–56] have found cyclic peptide variants to be less membrane-disrupting in antimicrobial or liposome leakage assays than the corresponding linear peptide variant. Most likely, the difference between the presently investigated peptides and these previous ones lies in the dominance in the present systems of conformational entropy effects (which promote adsorption of the cyclic peptide) and minor energetic cost of cyclization on peptide incorporation in the headgroup region, which are expected to be facilitated by readily expandable DOPE/DOPG membranes [52].

Various strategies have been employed to optimize the therapeutic index of AMPs, including use of combinational library approaches [57], stereoisomers composed of D-amino acids [58] or cyclic D,L-α-peptides [59], as well as QSAR and high-throughput based screening assays [60–64]. Furthermore, a novel approach for boosting AMPs through end-tagging with hydrophobic oligopeptide stretches was recently demonstrated [36,52,65,66]. In this context, the hydrophobic extension of NWC20c (NWCKRGRKQCKTHPHFVIPY) bears resemblence to the latter

Journal of PeptideScience

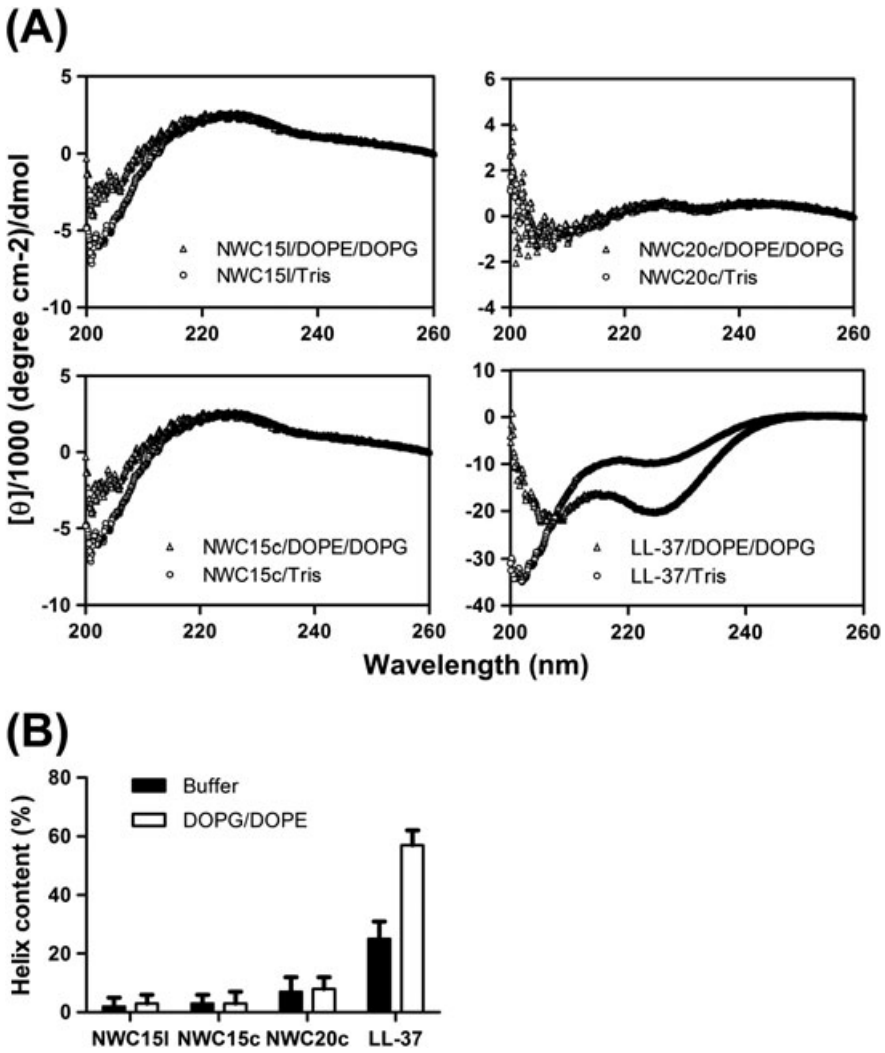

Figure 6. CD spectra (A) and helix content (B) for for the indicated peptides in 10 mM Tris, pH 7.4, with or without DOPE/DOPG (75/25 mol/mol) liposomes (100 μM lipid). LL-37 is shown for comparison.

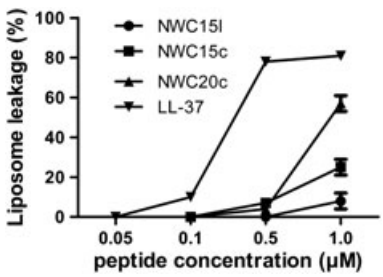

Figure 7. Peptide-induced liposome leakage for NWC15l, NWC15c, and NWC20c at 10 mM Tris, pH 7.4. Shown also are corresponding data for the benchmark peptide LL-37.

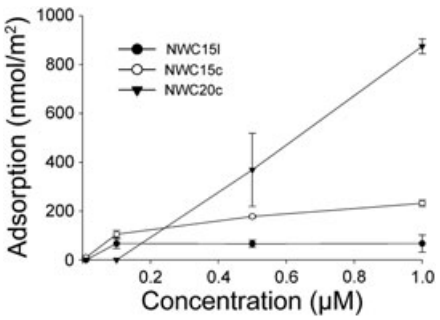

Figure 8. Adsorption of the indicated peptides to DOPE/DOPG (75/25 ml/mol) bilayers in 10 mM Tris, pH 7.4.

approach, leading to enhanced antimicrobial activity when compared with the peptide NWCKRGRKQCKTHPH. It should also be noted that because of potential lytic properties of AMPs against bacterial as well as mammalian membranes, a key challenge in designing new peptides relies on developing AMPs with high specificity against bacterial or fungal cells. The finding that the presently investigated APP peptides displayed no detectable lytic activities against mammalian cells under the conditions investigated makes them interesting as templates for further modification and variation in the investigation of AMP selectivity. Whether intact APP, or its extracellular and released heparin-binding N-terminal domain, exerts antimicrobial effects was not addressed in this study. However, it is worth noting in this context that APP is up-regulated in skin during wound healing. Whereas APP was predominantly expressed in the basal layer of unwounded skin, proliferating keratinocytes in all cell layers at the wound margin showed increased expression of APP [67]. Furthermore, APP gives rise to several bioactive fragments upon

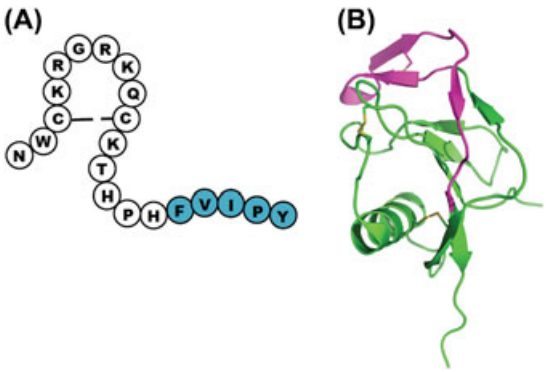

Figure 9. (A) Graphical illustration of the NWC peptides. The coloured FVIPY amino acid sequence indicates the hydrophobic extension. (B) Structure of the N-terminal domain of APP (PDB: 1MWP). The NWC20 region is indicated by pink color.

proteolysis [32]. Relevant to our results are also findings indicating that another region of APP, the Aβ peptide, has indeed been reported to exert antimicrobial activity [33], further delineating APP as a molecule containing regions coding for possible host defense functions. In contrast to the presently investigated peptides, however, Aβ is negatively charged and displays pronounced conformational transitions, resulting in peptide aggregation and fibrillation. Although membrane destabilization can be caused also by such structures (in analogy to membrane destabilization caused by, e.g. hydrophobic colloidal particles), such destabilization is fundamentally different from the local packing defects demonstrated in the present study. As a consequence of this, Aβ accumulation at, and destabilization of, lipid membranes is driven essentially by (lack of) colloidal stability of the peptide aggregates, hence does not differentiate between bacterial membranes and mammalian cell membranes, with considerable toxicity as a consequence [68,69]. The results in the present investigation of a more selective membrane action for the presently investigated region of APP further point to interesting antimicrobial properties of APP and peptide sequences thereof. Along with biophysical and biochemical data, the present work thus underscores the multifunctionality and multimodality of APP-derived peptides and suggests a role for the APP molecule in host defense.

Acknowledgements

This work was supported by grants from the Swedish Research Council (projects 13471 and 521-2009-3378), the Welander-Finsen, Thelma-Zoegas, Crafoord, Alfred Österlund, Lundgrens, and Kock Foundations, and The Swedish Government Funds for Clinical Research. We also wish to thank Ms Lotta Wahlberg and Ms Maria Baumgarten for expert technical assistance.

References

1 Yount NY, Bayer AS, Xiong YQ, Yeaman MR. Advances in antimicrobial peptide immunobiology. *Biopolymers* 2006; **84**: 435–458.
2 Zelezetsky I, Tossi A. Alpha-helical antimicrobial peptides-using a sequence template to guide structure-activity relationship studies. *Biochim. Biophys. Acta* 2006; **1758**: 1436–1449.
3 Tossi A, Sandri L. Molecular diversity in gene-encoded, cationic antimicrobial polypeptides. *Curr. Pharm. Des.* 2002; **8**: 743–761.
4 Powers JP, Hancock RE. The relationship between peptide structure and antibacterial activity. *Peptides* 2003; **24**: 1681–1691.
5 Bulet P, Stocklin R, Menin L. Anti-microbial peptides: From invertebrates to vertebrates. *Immunol. Rev.* 2004; **198**: 169–184.
6 Durr UH, Sudheendra US, Ramamoorthy A. LL-37, the only human member of the cathelicidin family of antimicrobial peptides. *Biochim. Biophys. Acta* 2006; **1758**: 1408–1425.
7 Brogden KA. Antimicrobial peptides: Pore formers or metabolic inhibitors in bacteria? *Nat. Rev. Microbiol.* 2005; **3**: 238–250.
8 Lohner K, Blondelle SE. Molecular mechanisms of membrane perturbation by antimicrobial peptides and the use of biophysical studies in the design of novel peptide antibiotics. *Comb. Chem. High Throughput Screen.* 2005; **8**: 241–256.
9 Beisswenger C, Bals R. Functions of antimicrobial peptides in host defense and immunity. *Curr. Protein Pept. Sci.* 2005; **6**: 255–264.
10 Yang D, Biragyn A, Hoover DM, Lubkowski J, Oppenheim JJ. Multiple roles of antimicrobial defensins, cathelicidins, and eosinophil-derived neurotoxin in host defense. *Annu. Rev. Immunol.* 2004; **22**: 181–215.
11 Elsbach P. What is the real role of antimicrobial polypeptides that can mediate several other inflammatory responses? *J. Clin. Invest.* 2003; **111**: 1643–1645.
12 Tjabringa GS, Ninaber DK, Drijfhout JW, Rabe KF, Hiemstra PS. Human cathelicidin LL-37 is a chemoattractant for eosinophils and neutrophils that acts via formyl-peptide receptors. *Int. Arch. Allergy Immunol.* 2006; **140**: 103–112.
13 Mookherjee N, Brown KL, Bowdish DM, Doria S, Falsafi R, Hokamp K, Roche FM, Mu R, Doho GH, Pistolic J, Powers JP, Bryan J, Brinkman FS, Hancock RE. Modulation of the TLR-mediated inflammatory response by the endogenous human host defense peptide LL-37. *J. Immunol.* 2006; **176**: 2455–2464.
14 Nordahl EA, Rydengard V, Nyberg P, Nitsche DP, Morgelin M, Malmsten M, Bjorck L, Schmidtchen A. Activation of the complement system generates antibacterial peptides. *Proc. Natl. Acad. Sci. U. S. A.* 2004; **101**: 16879–16884.
15 Nordahl EA, Rydengard V, Morgelin M, Schmidtchen A. Domain 5 of high molecular weight kininogen is antibacterial. *J. Biol. Chem.* 2005; **280**: 34832–34839.
16 Frick IM, Akesson P, Herwald H, Morgelin M, Malmsten M, Nagler DK, Bjorck L. The contact system--a novel branch of innate immunity generating antibacterial peptides. *EMBO J.* 2006; **25**: 5569–5578.
17 Pereira HA. Cap37, a neutrophil-derived multifunctional inflammatory mediator. *J. Leukoc. Biol.* 1995; **57**: 805–812.
18 Malmsten M, Davoudi M, Walse B, Rydengard V, Pasupuleti M, Morgelin M, Schmidtchen A. Antimicrobial peptides derived from growth factors. *Growth Factors* 2007; **25**: 60–70.
19 Pasupuleti M, Roupe M, Rydengard V, Surewicz K, Surewicz WK, Chalupka A, Malmsten M, Sorensen OE, Schmidtchen A. Antimicrobial activity of human prion protein is mediated by its N-terminal region. *PLoS One* 2009; **4**: e7358.
20 Nilsson M, Wasylik S, Morgelin M, Olin AI, Meijers JC, Derksen RH, de Groot PG, Herwald H. The antibacterial activity of peptides derived from human beta-2 glycoprotein i is inhibited by protein h and m1 protein from streptococcus pyogenes. *Mol. Microbiol.* 2008; **67**: 482–492.
21 Rydengard V, Shannon O, Lundqvist K, Kacprzyk L, Chalupka A, Olsson AK, Morgelin M, Jahnen-Dechent W, Malmsten M, Schmidtchen A. Histidine-rich glycoprotein protects from systemic candida infection. *PLoS Pathog.* 2008; **4**: e1000116.
22 Papareddy P, Rydengard V, Pasupuleti M, Walse B, Morgelin M, Chalupka A, Malmsten M, Schmidtchen A. Proteolysis of human thrombin generates novel host defense peptides. *PLoS Pathog.* 2010; **6**: e1000857.
23 Shooshtarizadeh P, Zhang D, Chich JF, Gasnier C, Schneider F, Haikel Y, Aunis D, Metz-Boutigue MH. The antimicrobial peptides derived from chromogranin/secretogranin family, new actors of innate immunity. *Regul. Pept.* 2010; **165**: 102–110.
24 Metz-Boutigue MH, Lugardon K, Goumon Y, Raffner R, Strub JM, Aunis D. Antibacterial and antifungal peptides derived from chromogranins and proenkephalin-a. From structural to biological aspects. *Adv. Exp. Med. Biol.* 2000; **482**: 299–315.
25 Papareddy P, Kalle M, Kasetty G, Morgelin M, Rydengard V, Albiger B, Lundqvist K, Malmsten M, Schmidtchen A. C-terminal peptides of tissue-factor pathway inhibitor are novel host defense molecules. *J. Biol. Chem.* 2010; **285**: 28387–28398.
26 Cardin AD, Weintraub HJ. Molecular modeling of protein-glycosaminoglycan interactions. *Arteriosclerosis* 1989; **9**: 21–32.
27 Andersson E, Rydengard V, Sonesson A, Morgelin M, Bjorck L, Schmidtchen A. Antimicrobial activities of heparin-binding peptides. *Eur. J. Biochem.* 2004; **271**: 1219–1226.

28 Ringstad L, Schmidtchen A, Malmsten M. Effect of peptide length on the interaction between consensus peptides and dopc/dopa bilayers. *Langmuir* 2006; **22**: 5042–5050.
29 Mattson MP. Cellular actions of beta-amyloid precursor protein and its soluble and fibrillogenic derivatives. *Physiol. Rev.* 1997; **77**: 1081–1132.
30 Leveugle B, Ding W, Durkin JT, Mistretta S, Eisle J, Matic M, Siman R, Greenberg BD, Fillit HM. Heparin promotes beta-secretase cleavage of the alzheimer's amyloid precursor protein. *Neurochem. Int.* 1997; **30**: 543–548.
31 Rossjohn J, Cappai R, Feil SC, Henry A, McKinstry WJ, Galatis D, Hesse L, Multhaup G, Beyreuther K, Masters CL, Parker MW. Crystal structure of the n-terminal, growth factor-like domain of Alzheimer's amyloid precursor protein. *Nat. Struct. Biol.* 1999; **6**: 327–331.
32 De Strooper B, Annaert W. Proteolytic processing and cell biological functions of the amyloid precursor protein. *J. Cell Sci.* 2000; **113**(Pt 11): 1857–1870.
33 Soscia SJ, Kirby JE, Washicosky KJ, Tucker SM, Ingelsson M, Hyman B, Burton MA, Goldstein LE, Duong S, Tanzi RE, Moir RD. The Alzheimer's disease-associated amyloid beta-protein is an antimicrobial peptide. *PLoS One* 2010; **5**: e9505.
34 Lehrer RI, Rosenman M, Harwig SS, Jackson R, Eisenhauer P. Ultrasensitive assays for endogenous antimicrobial polypeptides. *J. Immunol. Methods* 1991; **137**: 167–173.
35 Turner J, Cho Y, Dinh NN, Waring AJ, Lehrer RI. Activities of LL-37, a cathelin-associated antimicrobial peptide of human neutrophils. *Antimicrob. Agents Chemother.* 1998; **42**: 2206–2214.
36 Schmidtchen A, Pasupuleti M, Morgelin M, Davoudi M, Alenfall J, Chalupka A, Malmsten M. Boosting antimicrobial peptides by hydrophobic oligopeptide end tags. *J. Biol. Chem.* 2009; **284**: 17584–17594.
37 Malmsten M. Ellipsometry studies of protein layers adsorbed at hydrophobic surfaces. *J. Colloid Interface Sci.* 1994; **166**: 333–342.
38 Tiberg F, Harwigsson I, Malmsten M. Formation of model lipid bilayers at the silica-water interface by co-adsorption with non-ionic dodecyl maltoside surfactant. *Eur. Biophys. J.* 2000; **29**: 196–203.
39 De Feijter JA, Benjamins J, Veer FA. Ellipsometry as a tool to study the adsorption behavior of synthetic and biopolymers at the air–water interface. *Biopolymers* 1978; **17**: 1759–1772.
40 Malmsten M, Burns N, Veide A. Electrostatic and hydrophobic effects of oligopeptide insertions on protein adsorption. *J. Colloid Interface Sci.* 1998; **204**: 104–111.
41 Lotte K, Plessow R, Brockhinke A. Static and time-resolved fluorescence investigations of tryptophan analogues--a solvent study. *Photochem. Photobiol. Sci.* 2004; **3**: 348–359.
42 Glukhov E, Stark M, Burrows LL, Deber CM. Basis for selectivity of cationic antimicrobial peptides for bacterial versus mammalian membranes. *J. Biol. Chem.* 2005; **280**: 33960–33967.
43 Li X, Li Y, Peterkofsky A, Wang G. Nmr studies of aurein 1.2 analogs. *Biochim. Biophys. Acta* 2006; **1758**: 1203–1214.
44 Haney EF, Lau F, Vogel HJ. Solution structures and model membrane interactions of lactoferrampin, an antimicrobial peptide derived from bovine lactoferrin. *Biochimica et Biophysica Acta (BBA) - Biomembranes* 2007; **1768**: 2355–2364.
45 McInturff JE, Wang SJ, Machleidt T, Lin TR, Oren A, Hertz CJ, Krutzik SR, Hart S, Zeh K, Anderson DH, Gallo RL, Modlin RL, Kim J. Granulysin-derived peptides demonstrate antimicrobial and anti-inflammatory effects against propionibacterium acnes. *J. Invest. Dermatol.* 2005; **125**: 256–263.
46 Deslouches B, Phadke SM, Lazarevic V, Cascio M, Islam K, Montelaro RC, Mietzner TA. De novo generation of cationic antimicrobial peptides: Influence of length and tryptophan substitution on antimicrobial activity. *Antimicrob. Agents Chemother.* 2005; **49**: 316–322.
47 de Planque MR, Kruijtzer JA, Liskamp RM, Marsh D, Greathouse DV, Koeppe 2nd RE, de Kruijff B, Killian JA. Different membrane anchoring positions of tryptophan and lysine in synthetic transmembrane alpha-helical peptides. *J. Biol. Chem.* 1999; **274**: 20839–20846.
48 Andrushchenko VV, Vogel HJ, Prenner EJ. Interactions of tryptophan-rich cathelicidin antimicrobial peptides with model membranes studied by differential scanning calorimetry. *Biochim. Biophys. Acta* 2007; **1768**: 2447–2458.
49 Malmsten M, Davoudi M, Schmidtchen A. Bacterial killing by heparin-binding peptides from PRELP and thrombospondin. *Matrix Biol.* 2006; **25**: 294–300.
50 Jerala R. Synthetic lipopeptides: A novel class of anti-infectives. *Expert Opin. Investig. Drugs* 2007; **16**: 1159–1169.
51 Avrahami D, Shai Y. Conjugation of a magainin analogue with lipophilic acids controls hydrophobicity, solution assembly, and cell selectivity. *Biochemistry* 2002; **41**: 2254–2263.
52 Malmsten M, Kasetty G, Pasupuleti M, Alenfall J, Schmidtchen A. Highly selective end-tagged antimicrobial peptides derived from PRELP. *PLoS One* 2011; **6**: e16400.
53 Seker UO, Wilson B, Dincer S, Kim IW, Oren EE, Evans JS, Tamerler C, Sarikaya M. Adsorption behavior of linear and cyclic genetically engineered platinum binding peptides. *Langmuir* 2007; **23**: 7895–7900.
54 Ringstad L, Kacprzyk L, Schmidtchen A, Malmsten M. Effects of topology, length, and charge on the activity of a kininogen-derived peptide on lipid membranes and bacteria. *Biochim. Biophys. Acta* 2007; **1768**: 715–727.
55 Krishnakumari V, Sharadadevi A, Sitaram N, Nagaraj R. Consequences of introducing a disulfide bond into an antibacterial and hemolytic peptide. *J. Pept. Res.* 1999; **54**: 528–535.
56 Unger T, Oren Z, Shai Y. The effect of cyclization of magainin 2 and melittin analogues on structure, function, and model membrane interactions: Implication to their mode of action. *Biochemistry* 2001; **40**: 6388–6397.
57 Blondelle SE, Lohner K. Combinatorial libraries: A tool to design antimicrobial and antifungal peptide analogues having lytic specificities for structure-activity relationship studies. *Biopolymers* 2000; **55**: 74–87.
58 Sajjan US, Tran LT, Sole N, Rovaldi C, Akiyama A, Friden PM, Forstner JF, Rothstein DM. P-113 d, an antimicrobial peptide active against pseudomonas aeruginosa, retains activity in the presence of sputum from cystic fibrosis patients. *Antimicrob. Agents Chemother.* 2001; **45**: 3437–3444.
59 Fernandez-Lopez S, Kim HS, Choi EC, Delgado M, Granja JR, Khasanov A, Kraehenbuehl K, Long G, Weinberger DA, Wilcoxen KM, Ghadiri MR. Antibacterial agents based on the cyclic d,l-alpha-peptide architecture. *Nature* 2001; **412**: 452–455.
60 Hilpert K, Volkmer-Engert R, Walter T, Hancock RE. High-throughput generation of small antibacterial peptides with improved activity. *Nat. Biotechnol.* 2005; **23**: 1008–1012.
61 Taboureau O, Olsen OH, Nielsen JD, Raventos D, Mygind PH, Kristensen HH. Design of novispirin antimicrobial peptides by quantitative structure-activity relationship. *Chem. Biol. Drug Des.* 2006; **68**: 48–57.
62 Jenssen H, Lejon T, Hilpert K, Fjell CD, Cherkasov A, Hancock RE. Evaluating different descriptors for model design of antimicrobial peptides with enhanced activity toward p. *Aeruginosa. Chem Biol Drug Des* 2007; **70**: 134–142.
63 Pasupuleti M, Walse B, Svensson B, Malmsten M, Schmidtchen A. Rational design of antimicrobial C3a analogues with enhanced effects against staphylococci using an integrated structure and function-based approach. *Biochemistry* 2008; **47**: 9057–9070.
64 Fjell CD, Jenssen H, Cheung WA, Hancock RE, Cherkasov A. Optimization of antibacterial peptides by genetic algorithms and cheminformatics. *Chem. Biol. Drug Des.* 2011; **77**: 48–56.
65 Pasupuleti M, Chalupka A, Morgelin M, Schmidtchen A, Malmsten M. Tryptophan end-tagging of antimicrobial peptides for increased potency against Pseudomonas aeruginosa. *Biochim. Biophys. Acta* 2009; **1790**: 800–808.
66 Pasupuleti M, Schmidtchen A, Chalupka A, Ringstad L, Malmsten M. End-tagging of ultra-short antimicrobial peptides by W/F stretches to facilitate bacterial killing. *PLoS One* 2009; **4**: e5285.
67 Kummer C, Wehner S, Quast T, Werner S, Herzog V. Expression and potential function of beta-amyloid precursor proteins during cutaneous wound repair. *Exp. Cell Res.* 2002; **280**: 222–232.
68 Ittner LM, Gotz J. Amyloid-beta and tau--a toxic pas de deux in Alzheimer's disease. *Nat. Rev. Neurosci.* 2011; **12**: 65–72.
69 Aisenbrey C, Borowik T, Bystrom R, Bokvist M, Lindstrom F, Misiak H, Sani MA, Grobner G. How is protein aggregation in amyloidogenic diseases modulated by biological membranes? *Eur. Biophys. J.* 2008; **37**: 247–255.

